Journal of Non-Newtonian Fluid Mechanics 222 (2015) 104–111

Contents lists available at ScienceDirect

Journal of Non-Newtonian Fluid Mechanics

journal homepage: http://www.elsevier.com/locate/jnnfm

Gels formed from amino-acid derivatives, their novel rheology as probed by bulk and particle tracking rheological methods ☆

W.J. Frith [a,*], A.M. Donald [b], D.J. Adams [c], A. Aufderhorst-Roberts [d]

[a] Unilever R&D Colworth, Colworth Science Park, Sharnbrook, Bedfordshire MK44 1LQ, UK
[b] Cavendish Laboratory, Department of Physics, University of Cambridge, JJ Thomson Avenue, Cambridge CB3 0HE, UK
[c] Department of Chemistry and Centre for Materials Discovery, University of Liverpool, Crown Street, Liverpool L69 7ZD, UK
[d] School of Physics & Astronomy, E. C. Stoner Building, University of Leeds, Woodhouse Lane, Leeds LS2 9JT, UK

ARTICLE INFO

Article history:
Received 30 June 2014
Received in revised form 11 September 2014
Accepted 15 September 2014
Available online 28 September 2014

Keywords:
Rheology
Microrheology
Gel

ABSTRACT

We discuss the use of dynamic light scattering based particle micro-rheology to probe the lengthscale dependence of the microstructures formed by Fmoc-tyrosine gels. Past studies on these systems using dye diffusion have shown that Fmoc-tyrosine is capable of forming gels that can entrap molecules if they are large enough, unlike those gels formed by Fmoc-phenylalanine (Sutton et al., 2009). This result seems at odds with microscopic studies of the gel microstructure, which indicate porosity on much larger lengthscales than the molecular probes used. Here, we use particle probe based micro-rheology to investigate the porosity of the gels on larger lengthscales than is possible using molecular diffusion studies and show that there is considerable evidence of larger scale structures present in the gel. In particular we see that at no point does particle probe based micro-rheology reproduce the bulk properties of the gels, and also that there is strong dependence of the probe behaviour on particle size. Both of these results indicate the presence of microstructural features in the gel that are of the order of the particle size.

1. Introduction

Over the past decade and a half or so there has been a great deal of research published relating to hydrogels formed from the self-assembly of low molecular weight gelators (LMWGs), which typically comprise peptides or their derivatives with molecular weights less than 1 kDa. This interest has arisen for a number of reasons relating to application that include tissue repair, controlled release applications and novel ingredients in home and personal care products, for a recent overview of the subject, see Castillo-León et al. [2] and Zhao et al. [3].

It is vital in such applications to have a detailed understanding of the nature of the gel network in terms of both its microstructure and dynamics. Reported work on such systems reflects this particularly in terms of the microstructures formed, with many microscopy and scattering studies being published, as well as a number of recent reviews [4–7]. Information regarding the dynamics of the microstructure is less often reported, and is dominated by one technique in particular, which is the use of particle probe based microrheology (for a recent review see see Schultz and Furst [8]). This technique is particularly useful in the context of hydrogels for controlled release applications because it can explore the porosity and dynamics of the networks formed, which are key properties governing the materials' performance in terms of controlling the diffusion of active ingredients through the gel matrix. In particular the use of a range of probe particle sizes is proving to be a very interesting tool in characterising the microstructural lengthscales present in such gel matrices [9–13].

A very simple class of low molecular weight hydro-gelators are the Fmoc amino acids, specifically Fmoc-tyrosine (Fmoc-Y) and Fmoc-phenylalanine (Fmoc-F) (see Fig. 1 for structures), these readily form gels at low pH, whilst being soluble at high pH. Such materials are useful models for the formation and study of both the bulk and microstructural properties of their gels [1,14–16]. One of these studies [1] investigated the diffusion properties of a range of dyes in gels formed from Fmoc-F and Fmoc-Y, showing that the diffusion behaviour of the dyes in the gel matrix was dependent on molecular weight in the case of Fmoc-Y and not in Fmoc-F. The results are reproduced here in graphical form (see Fig. 2A) and show that in the case of Fmoc-Y, dye diffusion is cut-off at a molecular weight of around 1 kDa, which corresponds to around 1–4 nm in terms of the molecular size. In the case of Fmoc-F, there is no dependence of dye diffusion on molecular weight.

This difference in behaviour was ascribed to a hypothesised difference in the character of the gel network in the two samples.

☆ Dedicated to Prof Ken Walters FRS on the occasion of his 80th Birthday.

* Corresponding author. Tel.: +44 (0)1234222574.
E-mail address: bill.frith@unilever.com (W.J. Frith).

http://dx.doi.org/10.1016/j.jnnfm.2014.09.008
0377-0257/

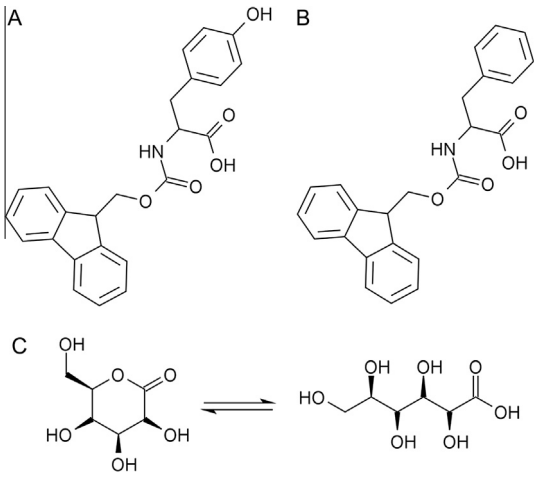

Fig. 1. (A) Fmoc tyrosine and (B) Fmoc phenylalanine chemical structures. (C) Glucono-δ-lactone (GdL) hydrolysis in water to form gluconic acid.

Rheological tests showed that Fmoc-F gels showed much stronger frequency dependence than the Fmoc-Y gels, and also that Fmoc-F gels were much more deformable that Fmoc-Y gels, failing at a strain of ∼100% and ∼1% for the Fmoc-F and Fmoc-Y gels respectively. These rheological results indicate that the Fmoc-F gels behave more like an entangled network of semi-flexible chains, whilst the Fmoc-Y gels form a network of rigid interconnections. This leads to a situation whereby diffusion through the Fmoc-F gels is determined by the relaxation dynamics of the network, whilst in the Fmoc-Y gels, diffusion is determined by the relative sizes of the dye molecules and the pore size of the network. Whilst this hypothesis seems to account for the different behaviour seen for the two gels, there is a discrepancy in the pore size implied by the diffusivity of the dye molecules, compared to that seen in cryo-SEM images of the gels (see Fig. 2B), which seems to imply that the mesh size is large enough to allow diffusion of particles significantly larger than the dye molecules used.

In addition to the dye diffusion work discussed above, both bulk rheological and microscopic particle tracking studies have been conducted on gels of Fmoc-Y [14–16], which explored how the kinetics of gelation and gel properties compared when measured using the two approaches. Comparison of the measured gel properties demonstrated that particle probes do not reproduce the bulk properties of the gels, implying that there must be microstructural features of the same order of lengthscales as the particles present in the gels. It thus appears that probe based measurements of the gel properties imply the presence of lengthscales in the gels from a few nanometres to nearly microns. In the following we explore this further using DLS based measurements of particle diffusion using a range of probe sizes and show that the Fmoc-Y based gels display gelation properties that are probe size dependent, again implying the presence of structures on the lengthscale of the particles, and much larger than implied by the dye diffusion measurements.

2. Materials and methods

2.1. Materials

N-(9-Fluorenylmethoxycarbonyl)-L-phenylalanine and N-(9-Fluorenylmethoxycarbonyl)-L-tyrosine (Fmoc-F and Fmoc-Y) were purchased from Sigma-Aldrich and used without further purification. Glucono-δ-Lactone (GdL) was obtained from Roquette and used as supplied. The tracer particles used in the DLS micro-rheology experiments were made of polystyrene with a negative charge on their surface and were obtained from Bangs Laboratories Inc.

2.2. Gel preparation

Following previous studies [1,17], uniform gels are produced by mixing a solution of the sodium salt of Fmoc-F or Fmoc-Y with an appropriate amount of GdL. The GdL hydrolyses gradually in solution to form gluconic acid (see Fig. 1C) and so produces a slow and uniform reduction in pH, allowing formation of uniform and reproducible gels.

Sodium salts of the Fmoc-amino-acids were prepared by neutralising a slight excess (∼5–10%) of either Fmoc-F or Fmoc-Y using a solution of NaOH at the desired volume and concentration (either 25 mM or 10 mM). For example, to prepare 10 ml of a 25 mM solution of Fmoc-Y, 110 mg (0.27 mmol) of Fmoc-Y were added to 10 ml of 25 mM NaOH. The mixture was then repeatedly warmed and dispersed (using an ultrasound bath) until the pH had dropped to 8.5. At this point the concentration of the sodium salt of Fmoc-Y should be equal to the concentration of the original NaOH solution. The excess undissolved Fmoc-Y was removed using a 0.2 μm syringe filter.

Having prepared the solution of the sodium salt of the Fmoc-amino acid, the gel was then prepared by adding GdL to the solution in an amount that ranged between 6 and 18 mM. The hydrolysis of the GdL is sufficiently slow that complete dissolution and subsequent handling of the mixture is possible prior to gelation, allowing the loading of the sample into a rheometer or light scattering apparatus.

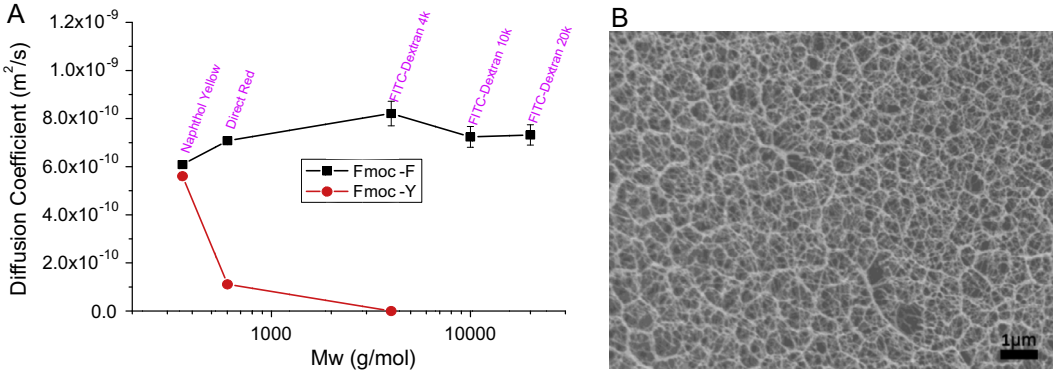

Fig. 2. (A) Molecular weight dependence of the diffusion coefficient of a range of dyes in Fmoc-F and Fmoc-Y gels. (B) cryo-SEM image of an Fmoc-Y gel. Data reproduced in graphical form from [1].

2.3. Bulk rheology

Bulk rheological experiments were carried out using an Anton-Paar MCR501 rheometer equipped with a serrated concentric cylinder geometry (the serrations serve to eliminate wall slip effects). After mixing the ingredients to prepare the gel, the sample was introduced into the measuring geometry and the measurement started as rapidly as possible (within 1 min). In order to monitor gelation, the dynamic moduli (G' and G'') were measured at 1 Hz and 0.1% strain every minute for 20hrs. After this, the resulting gel was characterized using a frequency sweep at 0.1% strain followed by a strain sweep at 1 Hz. The samples were covered with a layer of light mineral oil to prevent water loss.

2.4. Micro-rheology

The dynamic light scattering measurements were conducted using an ALV CGS-8F goniometer equipped with an LSE-5003 digital correlator with dual avalanche photodiode detectors operated in cross-correlation mode and a 30mW HeNe laser. 10 mm disposable glass cuvettes were used in all cases.

The tracer particles used were obtained from Bangs Laboratories Inc and comprised poly(styrene) spheres with diameters of 0.12, 0.52 and 1.01 μm as quoted by the manufacturer. The hydrodynamic radii, as measured by dynamic light scattering were 0.073, 0.365 and 0.771 μm.

Because DLS requires that only single scattering events occur in the sample there is a maximum concentration of tracer particles that can be used, also, in order to minimize effects from background scattering of the sample it is desirable to use as high a concentration of tracer particles as possible. To this end a series of DLS measurements of the size of the particles as a function of concentration were used to determine the maximum possible concentration of particles that could be used, this was determined to be 0.001% w/w, and this concentration was used in all measurements reported here.

Gelation studies were conducted in a manner similar to the rheological studies. Samples were prepared in the same manner, placed in the cuvette in the light scattering apparatus, and measurements started within 1 min. Gelation of the sample was monitored by recording the autocorrelation function for 60 s at an angle of 40° repeatedly for a period of 20 h, which resulted in one measurement being made every 84 s.

Mean squared displacements (MSDs) of the probe particles were determined from the intensity correlation function following the approach of Schätzel et al. [18] and Oppong et al. [19]. The MSD is directly related to the field autocorrelation function $g^{(1)}(\tau)$ which is in turn related to the measured intensity autocorrelation function $g^{(2)}(\tau)$ via the following.

$$g^{(1)}(\tau) = 1 + \frac{\langle I\rangle_T}{\langle I\rangle_E}\left[\sqrt{1 + \frac{g^{(2)}(\tau) - g^{(2)}(0)}{\beta}} - 1\right] \quad (1)$$

where I_T is the time average scattering intensity for the measurement and I_E is the ensemble average scattering intensity, which is assumed to be the same as I_T measured for the same sample, but before gelation has occurred. β is a correction factor determined from the intercept of $g^{(2)}(\tau)$ at $\tau = 0$ for the un-gelled sample.

The MSD can then be calculated from

$$\langle r^2(\tau)\rangle = \frac{-6ln(g^{(1)}(\tau))}{q^2} \quad (2)$$

where the scattering vector $q = (4\pi n/\lambda)\sin(\theta/2)$, n is the refractive index of the solvent, λ is the wavelength of the incident light, and θ is the scattering angle. The data for $g^{(2)}(\tau)$ are only reliable for values above ~0.01, which corresponds to an MSD of approximately 10^{-13} m^2, although this level is rather dependent on the size of the probe particles.

3. Results and discussion

3.1. Bulk rheology

Gels formed by Fmoc-F and Fmoc-Y differ in a number of respects; in particular Fmoc-F gels seem to form more quickly and are less stable than Fmoc-Y gels. In the previous studies of dye diffusion within these two gels, the conditions at which the gels formed were different. Fmoc-F gels were formed from 25 mM Fmoc-F and 6 mM GdL, whilst Fmoc-Y gels were formed at 25 mM Fmoc-Y and 18 mM GdL. This was because stable Fmoc-F gels could not be produced at the higher GdL concentrations used for the Fmoc-Y gels. One consequence of the preparation conditions used was that Fmoc-F gels would not have been fully converted to the acid form, since there was not a stoichiometric amount of GdL present. Conversely, it is likely that most of the Fmoc-Y was converted to the acid form. The ability of Fmoc-Y to form stable gels at higher GdL concentrations appears to be due to the presence of the OH group on the phenyl ring (which is the only structural difference between Fmoc-Y and Fmoc-F) leading to additional stabilisation of the self-assembled fibrils via hydrogen bonding.

The question arises of just how different are the gels formed from the two compounds. Clearly the two gels are very different as studied previously, but these were formed under different gelation conditions. We now explore how the properties of the gels, and those formed from Fmoc-Y in particular, depend on gelation conditions by varying the concentrations of the GdL and the Fmoc-Y. Fig. 3 shows the gelation behaviour at 25 mM of Fmoc-Y, with the concentration of GdL varied from 6 mM to 18 mM. Also shown in Fig. 3 for comparison is the gelation response of Fmoc-F at the same conditions as previously studied [1] (25 mM Fmoc-F & 6 mM GdL). Fig. 4 and 5 show the corresponding frequency and strain responses of the final gels, each figure also shows the behaviour of the Fmoc-F gel.

From Fig. 3 it is clear that both the type of gelator and the concentration of GdL have a strong influence on the kinetics of gelation. The Fmoc-F solution gels more rapidly that any of the Fmoc-Y samples, forming a measureable elastic response at the earliest measurement times, and gelling (as measured by the time

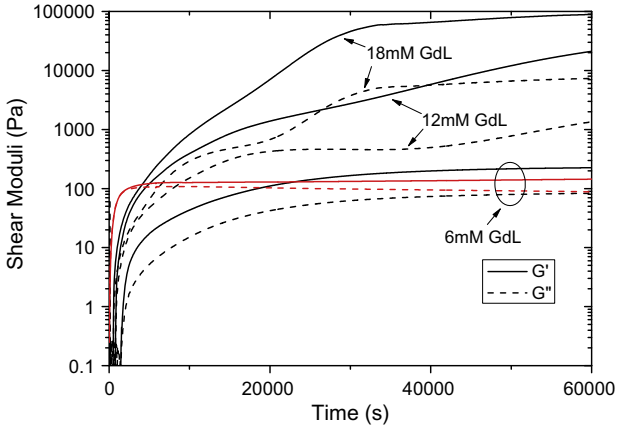

Fig. 3. Time dependence of storage (solid lines) and loss (dashed lines) moduli for 25 mM Fmoc-F with 6 mM GdL (red) and 25 mM Fmoc-Y in 6 mM, 12 mM and 18 mM GdL (black) (moduli increase in magnitude with GdL concentration). (For interpretation of the references to colour in this figure legend, the reader is referred to the web version of this article.)

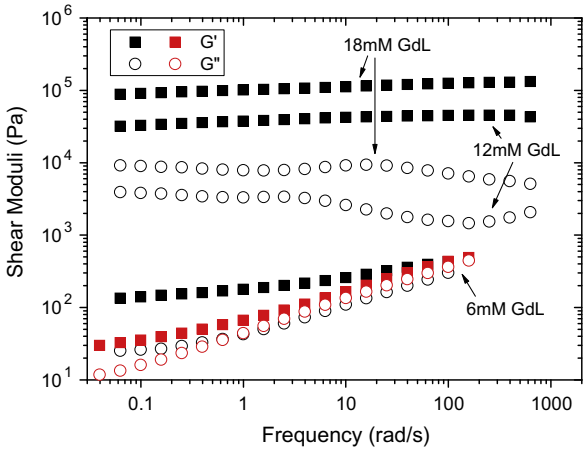

Fig. 4. Frequency dependence of storage (solid squares) and loss (open circles) moduli for 25 mM Fmoc-F with 6 mM GdL (red) and 25 mM Fmoc-Y in 6 mM, 12 mM and 18 mM GdL (black) (moduli increase in magnitude with GdL concentration). (For interpretation of the references to colour in this figure legend, the reader is referred to the web version of this article.)

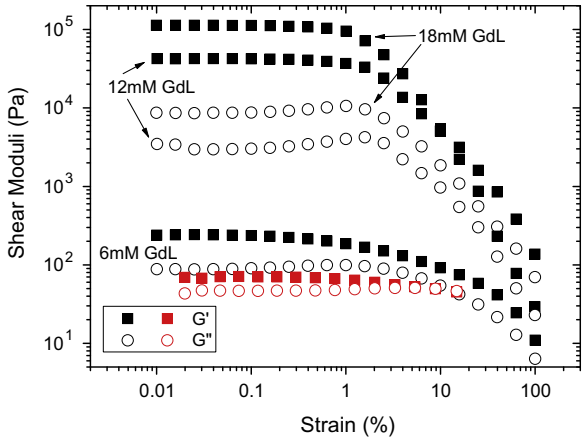

Fig. 5. Strain dependence of storage (solid squares) and loss (open circles) moduli for 25 mM Fmoc-F with 6 mM GdL (red) and 25 mM Fmoc-Y in 6 mM, 12 mM and 18 mM GdL (black) (moduli increase in magnitude with GdL concentration). (For interpretation of the references to colour in this figure legend, the reader is referred to the web version of this article.)

at which G' becomes greater than G'') in approximately 600 s. In contrast, the Fmoc-Y solutions display a pronounced lag time before a measurable elastic response is observed, gelation appears to occur very close to the time that the first elastic response is measured. The observed lag times were: 510, 810 and 1470 s for the 18, 12 and 6 mM GdL samples respectively. As the gelation process continues, the Fmoc-F reaches an approximate plateau in properties with time after approximately 5000 s and then remains relatively unchanged for the remainder of the gelation period up to 60,000 s. The Fmoc-Y gels take much longer to reach an apparent plateau in properties, at least 40,000 s and in one case (the 12 mM GdL sample) no plateau is reached during the experiment. In the case of the 6 mM GdL sample, the final gel modulus is similar to that of the Fmoc-F gels, although the gel takes much longer to form. At higher levels of GdL, the stiffness of the gels increases dramatically with the 18 mM GdL sample reaching a plateau G' of ~100,000 Pa compared to ~100 Pa for the 6 mM GdL samples. It also appears that the higher concentrations of GdL lead to more complex gelation kinetics. For the 12 and 18 mM GdL samples, the moduli initially display a downward curvature with time up to about 20,000 s; at later times the rate of increase of the moduli accelerates for a period and then resumes a slowly decreasing rate until an apparent plateau is finally reached. The clear implication of this behaviour is that there are two processes involved in the formation of the Fmoc-Y gels at higher GdL concentrations, this is discussed further below.

Fig. 4 shows the frequency response of the final gels formed from both Fmoc-F and Fmoc-Y. As with the gelation kinetics, the two gelators display quite distinct behaviours. At high GdL concentrations the Fmoc-Y samples display only a weak dependence of G' on frequency and large values compared to the 6 mM GdL samples. Such behaviour indicates the formation of a permanent, strong gel. At a GdL concentration of 6 mM, both the Fmoc-Y and Fmoc-F samples display G' values in the region of 100 Pa, some 2–3 orders of magnitude lower than the two higher concentrations of GdL. However, the two gelators do display differing behaviour at 6 mM GdL concentration, whilst the Fmoc-Y still only displays a weak dependence of G' on frequency, the Fmoc-F sample displays a relatively strong frequency dependence. This different in behaviour is consistent with the Fmoc-Y sample possessing a more permanent network than the Fmoc-F sample.

The strain dependence of the elastic moduli, shown in Fig. 5, supports the idea that there is a different type of network present in the gels formed at 6 mM GdL concentrations. Whilst the higher concentrations of GdL form gels that are rather brittle, displaying failure at a strain of around 1%, at 6 mM GdL both of the gelators form gels that are far more deformable. In particular, the gels appear to be able to withstand large strains without irreversible breakdown. Such behaviour is characteristic of a sparsely cross-linked network of flexible chains, and may also be characteristic of an entangled network of flexible chains. On the other hand, the behaviour seen at higher GdL concentrations is characteristic of a densely cross-linked network of relatively rigid links or rods.

In summary, it appears that the gels formed at 6 mM GdL show a distinctly different character to those formed at the two higher GdL concentrations. The differences can be rationalised by hypothesising a more densely cross-linked network of stiff chains or rods at higher GdL concentrations, whilst at 6 mM GdL the gel behaviour is akin to that of a very sparsely cross-linked network of flexible chains, or an entangled network. This difference in behaviour may arise from the different levels of neutralisation of the sodium salts of the Fmoc amino acids. At higher GdL concentrations, there is a relatively high degree of neutralisation, and the fibrils forming the network should be relatively uncharged. This appears to lead to aggregation of fibrils into larger bundles during the later stages of gelation, leading to a dense network with rod-like interconnections that is apparently revealed through cryo-SEM (see Fig. 2B). At lower GdL concentrations there is sufficient residual charge on the fibrils to prevent them from associating, and so the lateral aggregation process described above does not occur, and the resulting gel structure resembles that of an entangled network of flexible or semi-flexible chains.

These data are in accordance with those measured previously when investigating the dye release behaviour of the gels [1], however, by investigating a broader GdL concentration range we see that there appears to be a common basis to the gelation behaviour of the two gelators. It is worth noting that behaviour similar to this has been observed in other, related gelators based on bromo-naphthalene di-peptides, where gels formed using GdL were much stiffer than those formed at a higher pH using CO_2 [20], which were much more flexible.

In the following we explore the use of DLS based micro-rheology to follow the development of the gel network in Fmoc-Y gels,

and also to probe the lengthscale dependence of the properties as measured using probe particle diffusion.

3.2. Micro-rheology

So as to facilitate the study of Fmoc-Y gels using tracer particle micro-rheology, a composition was selected that had a low modulus and long gelation time. This had two main benefits; the long gelation time facilitated sample handling, whilst the low modulus enabled more extensive studies to be undertaken, since particle diffusion based microrheology suffers from the limitation that in stiff materials the particle motion can become too small to detect. Additionally, as discussed below, reducing the concentration enhances the contrast between the gel and the tracer particles. To this end it was decided to conduct measurements using an Fmoc-Y concentration of 10 mM and a GdL concentration of 10 mM, initially.

In order for DLS based micro-rheology to be successful, there must be sufficient scattering contrast between the sample and the tracer particles. In order to achieve this, the maximum possible concentration of tracer particles was added such that single scattering events still dominated (as determined by measurements of diffusion coefficients in water at different concentrations). In order to determine whether or not the background scattering from the sample was sufficiently low compared to that of the tracer particles, we also compared the scattering intensities obtained from samples with and without tracer particles as a function of time. The results of this exercise are shown in Fig. 6. From this figure it can be seen that although initially the scattering from the sample without tracer particles is low compared to those containing tracer particles, as gelation proceeds this eventually ceases to be the case. This is presumably because of the development of supra-molecular structures, such as those seen previously (Fig. 2B). Based on the results in Fig. 6 it was decided to only use data collected in the first 240 min of the experiment, after which point the scattering from the gel network became rather too large to ignore.

Fig. 7 shows the development of the MSDs for the three bead sizes used in this study as a function of time as the gel develops. These results show the behaviour expected for a sample that is undergoing a transition from a low viscosity Newtonian fluid to a viscoelastic solid. Specifically the early MSDs show a power law slope of one, indicating a Newtonian fluid. The first change observed is that after a delay, the MSDs move to lower values, whilst the slope remains the same, indicating an increase in viscosity, but still Newtonian behaviour. Next, the slope then begins to decrease in addition to the decreasing magnitude; a slope less than one indicates the development of a viscoelastic response. At later

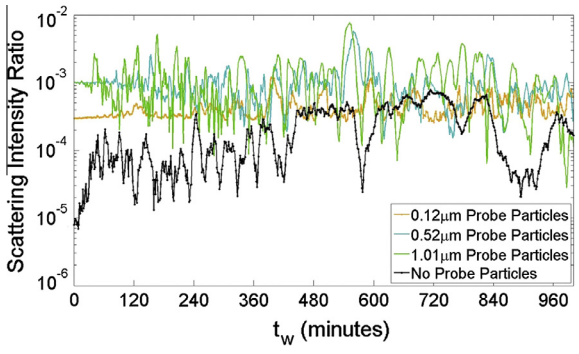

Fig. 6. Time dependence of scattering intensity from samples with the three different size tracer particles, compared with the scattering intensity from the sample without tracer particles.

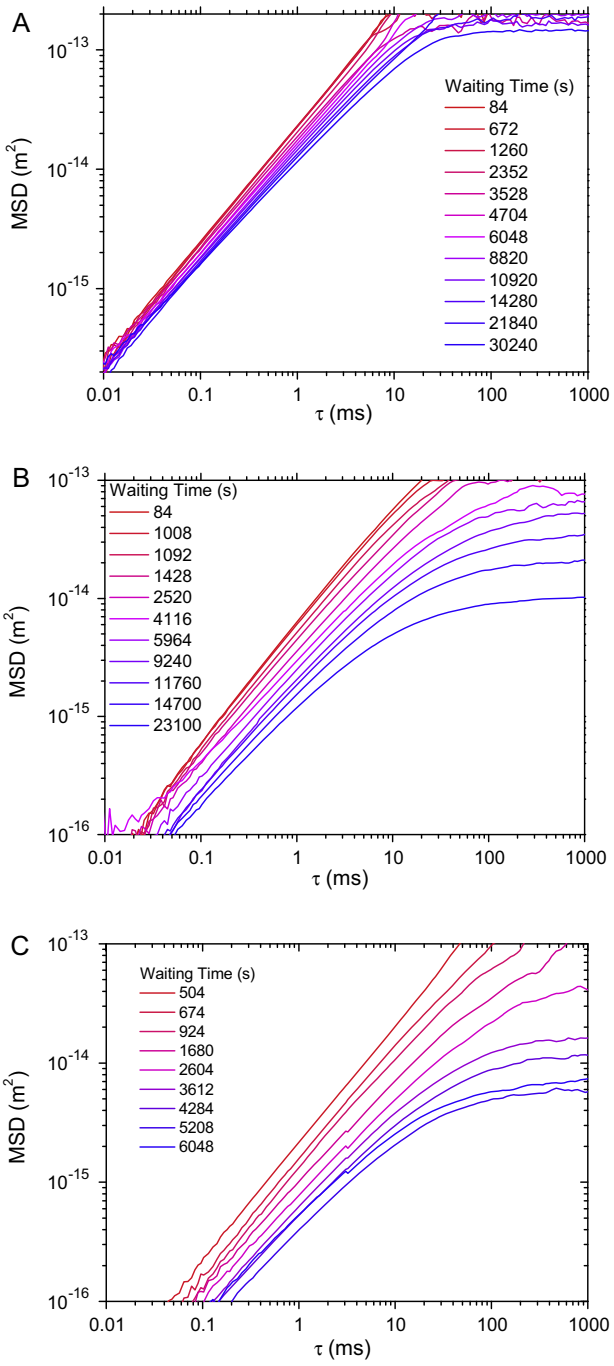

Fig. 7. Mean squared displacements of tracer particles as a function of delay time (τ) for samples at different times after adding GdL, as measured by dynamic light scattering. (A) 0.12 μm, (B) 0.52 μm and (C) 1.01 μm nominal tracer particle diameters.

times the MSDs begin to display a downward curvature. This behaviour implies that there is a limiting lengthscale for the diffusion of the tracer particles, and that they are trapped within a gel network. Finally, the slope of the MSD at large τ reaches approximately zero, confirming the entrapment of the particles.

MSD data has been used in the past to determine the gel point unambiguously by shifting the individual MSD plots, obtained during the gelation process, horizontally and vertically so that they fall onto two master curves, one for the pre-gel network, and one for the post-gel network [21,22]. This is possible because MSDs obtained in an un-gelled system must tend to a power-law slope

of one, and so will show a zero or positive 2nd derivative of the MSD on a log-log scale. Post gelation the MSDs, on the other hand, must tend to a plateau because the particles are by definition trapped, and so the 2nd derivative of the MSD with respect to τ will be negative. Unfortunately, for these gelling systems, the light scattering method does not allow determination of the MSD to large enough values to allow this scaling to be conducted. However, these data allow us to define two key parameters relating to the developing gel network, namely, the time at which the observed MSD begins to decrease in magnitude, and the time at which a plateau in the MSD is first observed.

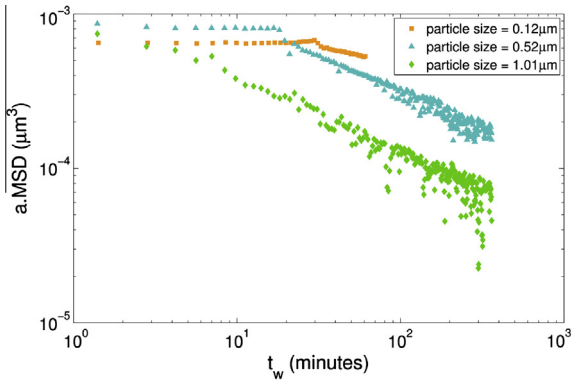

Fig. 8. MSD at a delay time (τ) of 1 ms as a function of time after adding GdL. Values are normalised by the particle radius (a).

Whilst the gel time has been investigated in the past [16,21,22], the time at which the MSDs first begin to change has received less attention. The onset of the shift in MSD at early times is illustrated in Fig. 8 where the MSD at a delay time of 1 ms is plotted as a function of time from the start of the experiment. In this figure the MSD has been normalised by the particle radius, so that the resulting values should be the same for all particle sizes at the start of the experiment. We see in all cases that, after an initial delay, the particle diffusion begins to decrease, also the time at which this occurs is strongly particle size dependent, with the larger particles showing a decrease in MSD more quickly than the smaller particles.

The strong dependence of the delay time on particle size appears to signify the presence of relatively large-scale structures in the sample (of the order of the particle size), that are present at a very early stage of the self assembly process, significantly before gelation occurs.

It is also interesting to consider the development of the plateau in the MSDs as a function of time after the start of the experiment. This is shown in Fig. 9A where the evolution of the mean MSD between $1 < \tau < 30$ s is shown. In this figure, data are binned and averaged over 5 measurements (or 10 in the case of the 120 nm particles). As mentioned earlier, there is an upper limit to the precise determination of MSDs that arises because $g^{(2)}(\tau)$ values below 0.01 cannot be measured accurately. As a result there is a noise limited ceiling to the MSD that is in the region of $1–2 \cdot 10^{-13}$ m^2, depending on the tracer particle size.

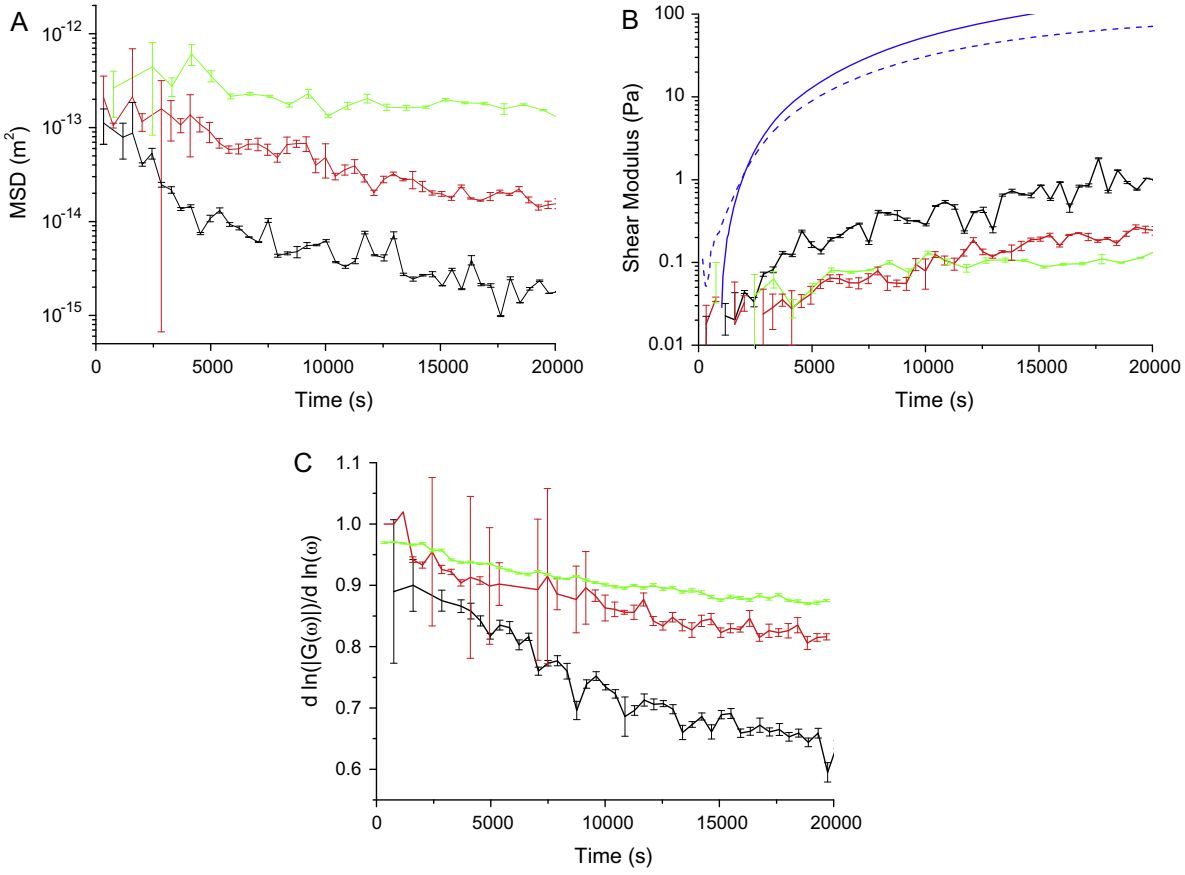

Fig. 9. (A) MSDs averaged over delay times (τ) 1–30 s as a function of time after adding GdL. (Black) 1.01 μm, (red) 0.52 μm, (green) 0.12 μm nominal tracer particle sizes. Data are also averaged over 5 measurements (1.01 μm & 0.52 μm) or 10 measurements (0.12 μm). (B) Plateau moduli determined from MSD values in (A) colours are same as for (A). Blue lines are bulk rheology measurements of the storage (solid line) and loss (dashed line) moduli for the same sample. (C) Logarithmic slopes of the complex modulus ($|G(\omega)|$ for $103 < \omega < 104$ rad/s) as a function of time, colours are the same as for (A) all data are averages of 5 measurements. (For interpretation of the references to colour in this figure legend, the reader is referred to the web version of this article.)

When the particle MSDs display a plateau with τ, the elastic modulus of the network as perceived by the probe particles can be determined straightforwardly:

$$G = \frac{kT}{\pi a \langle r^2_{plateau} \rangle} \tag{3}$$

where G is the shear modulus, k is the Boltzmann constant, T is the temperature, a is the particle radius and $r^2_{plateau}$ is the MSD for $1 < \tau < 30$ s. Fig. 9B shows the time evolution of this modulus, for the three probe particle sizes, as well as that of the bulk modulus measured using conventional rheometry. This figure clearly shows that there is a strong dependence of the modulus measured using probe particles on their size. Also, all the moduli measured using micro-rheological approaches fall well below those measured using conventional rheology for this particular system, which undoubtedly reflects the rather coarse microstructure of the gels when compared to the size of the particles. Such behaviour is known to occur in gels that have coarse microstructures [23–25], which can lead to the local environment surrounding the particles being significantly different to the bulk properties. If the probe particles do not interact with the gel medium then the immediate environment surrounding individual particles will, through simple steric arguments, allow greater freedom for the particle to diffuse than would be implied by bulk properties of the gel. Thus the observation that the elastic modulus measured using probe particles is lower than the bulk measurement is not surprising, and also confirms that the particle do not interact with in any specific way with the gel network. In hydrodynamic terms, such behaviour results from the breakdown of the Stokes-Einstein relationship, which assumes that the medium in which the particles are suspended is uniform on lengthscales significantly smaller the those of the particles, for a recent review on the subject, see Squires and Mason [23].

One advantage of the scattering based micro-rheological approach is that it is feasible to investigate the rheological properties of samples at much higher frequencies than is possible using bulk approaches. This allows comparison of the data with models for the dynamics of polymer networks which predict power law dependences of the elastic moduli on frequency (ω) of 1/2–2/3 for flexible chains (Rouse and Zimm models) or 3/4 for semi-flexible chains [26–28]. In the high frequency region of the viscoelastic spectrum it is expected that G', G'' and $|G|$ (respectively the storage, loss and complex moduli) should all show the same power law dependence. To this end we calculated $|G(\omega)|$using the approach of Mason [29] whereby:

$$|G(\omega)| = \frac{k_B T}{\pi a \langle r^2(1/\omega) \rangle \Gamma(1 + \alpha(\omega))} \tag{4}$$

where

$$\alpha(\omega) = \left. \frac{d \ln \langle r^2(\tau) \rangle}{d \ln \tau} \right|_{\tau = 1/\omega}$$

The slope ($d \log |G(\omega)| / d \log \omega$) was calculated for $10^3 < \omega < 10^4$ and is shown in Fig. 9C. It is evident from this figure that, as with the plateau moduli, there is a very strong dependence of the behaviour on the probe particle size. As expected, at early times all the slopes are close to 1 indicating that the solution is a Newtonian medium. At later times the slopes decrease; for the two smaller probe particle sizes the decrease is only slight, for the 1 μm probe particles however, the slope eventually drops to approximately 0.65, consistent with a network of flexible Zimm chains [26]. Similar studies on biopolymers such as actin [30] and pectin [31] have previously observed semi-flexible dynamics (i.e. a $|G(\omega)|$ power law of 3/4) clearly different behaviour from that observed here. It is puzzling that we observe this behaviour in the light of the microstructure seen in SEM images and the observed particle size dependence of the results, both of which imply that the microstructure of the gels is characterised by supramolecular lengthscales of the order of several 100 s of nm. This result may imply the presence of a hierarchical microstructure of a coarse grained network (seen in cryo-SEM) embedded in a solution of flexible self-assembled chains that is invisible to SEM. It should be noted however, that this is currently speculation and should be treated with caution.

This result also highlights the importance of using a range of probe particle sizes to conduct micro-rheological experiments. Clearly, the behaviour is very dependent on the probe particle radius and, besides shedding light on the micro-structural lengthscales in gels such as these, using multiple probe particle sizes avoids the risk of drawing erroneous conclusions from measurements using a single particle size.

In order to further characterise the gelation kinetics, the time at which a clear, low noise, plateau first appears was determined by visual inspection of the MSDs and is shown in Fig. 10 (a more quantitative approach was not possible due to the rather noisy nature of the data). For the two larger particle sizes this could be determined relatively unambiguously, and corresponds roughly with the intersection of the initial slope of the plateau MSD with time and the noise ceiling for the MSD. For the smallest particle size, the plateau remained relatively close to the limit of measurability, although, as can be seen from Fig. 9A, and the plots of MSD versus τ in Fig. 7A, a clear plateau did form. This meant that determining the time at which the plateau emerged was difficult and the analysis of the data should be treated with caution.

The times at which the MSD at $\tau = 1$ ms begins to decrease are also shown in Fig. 10. The particle size dependence for this and for the time of emergence of a plateau in MSD is similar in this figure, indicating that microstructure of similar lengthscales as the particles is present at all times, rather than developing at some later stage. This conclusion follows directly from the principle that a particle size dependence of diffusion behaviour is only observed if the generalised Stokes-Einstein relation breaks down in some manner [23]. There are a number of possible reasons for this happening in general, but it is known to happen in gels, where the microstructural lengthscales can be of the same order as the probe particle size. In extreme cases this can lead to particles being trapped or free to diffuse, depending on their size [23–25]. Hence, it follows that such structures a very likely to be present if a particle size dependence of the diffusion is observed. That such behaviour is seen prior to gelation may imply that nuclei, forming very

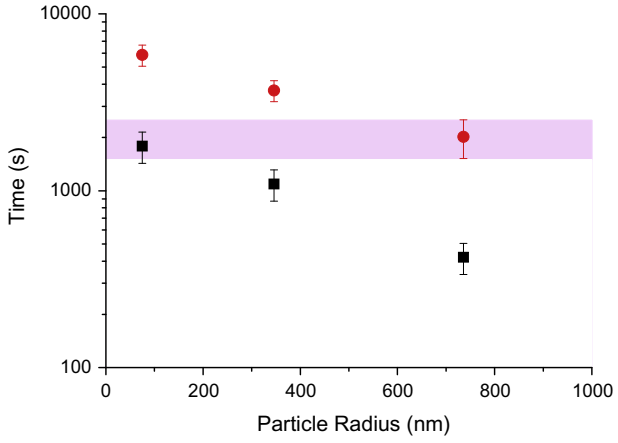

Fig. 10. Tracer particle size dependence of the times for the first measurable decrease in MSD at $\tau = 1$ ms (black squares) and the earliest appearance of a clear plateau in MSD (red circles). Shaded region represents the gelation time for the same sample measured using bulk rheology. (For interpretation of the references to colour in this figure legend, the reader is referred to the web version of this article.)

early in the self-assembly process, rapidly grow to a large size, long before gelation has actually occurred.

Also shown in Fig. 10 is the gelation time for the sample as measured using bulk rheology. It is worth noting that the times of appearance of the plateau MSDs are in general greater than the gelation time measured using bulk rheology, although the largest probe size is approximately equal to the bulk measurement. It seems reasonable to assume that even larger particle sizes should behave in the same manner as for the 1.01 μm tracer particles, since it would not be expected that a plateau in MSD develops before gelation had occurred, and the 1.01 μm particles already display a plateau at the measured gelation time. The values of the times for the initial decrease in MSD are less than the bulk rheology gelation time, except for the smallest tracer particle size, which is approximately equal to the bulk measurement. It might be expected that a tracer particle would sense a change in the material properties prior to gelation, no matter how small is was, however, this is apparently not the case in these experiments. In the light of these data it would be interesting to conduct further studies over a wider range of probe sizes than used here.

4. Conclusions

We have used a combination of rheological methods to explore the gelation behaviour and microstructure of Fmoc-tyrosine gels. Particle probe based investigations appear to indicate that the gel possesses features with lengthscales on the order of microns, and this is borne out by cryo-SEM studies. This result is in intriguing contrast to our earlier data showing the entrapment of molecular dyes in the gel [1]. An analysis of the high frequency viscoelastic response of the gels also implies that there may be a flexible network of Zimm-like chains, rather than a semi-flexible network as has been observed previously in biopolymers [30,31]. The existence of a Zimm-like response in the gels may imply the existence of a finer grained microstructure than in implied by the cryo-SEM data. This apparent contradiction may imply that the gel network exists on a broad range of lengthscales, from the molecular to micron sized, and that the smaller lengthscales are invisible using techniques such as SEM. Further studies will be needed to confirm such a hypothesis, however.

When the benefits and drawbacks of the use of probe based diffusion measurements to characterise gels are considered in comparison to other techniques such as rheology and microscopy it is striking that such techniques are highly complementary. For instance scattering based approaches to micro-rheology offer access to frequency ranges not accessible to other methods. In contrast microscopic particle tracking approaches offer the abilities to investigate sample heterogeneity [15,32] or to track the longer timescale behaviour of particles that allows observation of such phenomena as anomalous diffusion and cage-hopping [33]. Each technique offers insights not provided by the other. As such it is very important to consider carefully the questions one is asking before choosing the techniques to apply.

Acknowledgements

Parts of this work are drawn from the doctoral thesis of A.A-R, for which the authors gratefully acknowledge funding from the EPSRC and Unilever R&D Colworth through an EPSRC CASE studentship. The authors also gratefully acknowledge the helpful comments of the reviewers in relation to analysing the high frequency properties of the samples.

References

[1] S. Sutton, N.L. Campbell, A.I. Cooper, M. Kirkland, W.J. Frith, D.J. Adams, Controlled release from modified amino acid hydrogels governed by molecular size or network dynamics, Langmuir 25 (2009) 10285–10291.
[2] J. Castillo-León, L. Sasso, W.E. Svendsen, Self-assembled Peptide Nanostructures: Advances and Applications in Nanobiotechnology, Pan Stanford Publishing Pte. Ltd., 2012.
[3] X. Zhao, F. Pan, H. Xu, M. Yaseen, H. Shan, C.A.E. Hauser, S. Zhang, J.R. Lu, Molecular self-assembly and applications of designer peptide amphiphiles, Chem. Soc. Rev. 39 (2010) 3480–3498.
[4] A. Dasgupta, J.H. Mondal, D. Das, Peptide hydrogels, RSC Adv. 3 (2013) 9117–9149.
[5] I.W. Hamley, Self-assembly of amphiphilic peptides, Soft Matter 7 (2011) 4122–4138.
[6] C. Yan, D.J. Pochan, Rheological properties of peptide-based hydrogels for biomedical and other applications, Chem. Soc. Rev. 39 (2010) 3528–3540.
[7] D.J. Adams, P.D. Topham, Peptide conjugate hydrogelators, Soft Matter 6 (2010) 3707–3721.
[8] K.M. Schultz, E.M. Furst, Microrheology of biomaterial hydrogelators, Soft Matter 8 (2012) 6198–6205.
[9] Q. Lu, M.J. Solomon, Probe size effects on the microrheology of associating polymer solutions, Phys. Rev. E 66 (2002) 061504/1–061504/11.
[10] B.R. Dasgupta, S.Y. Tee, J.C. Crocker, B.J. Frisken, D.A. Weitz, Microrheology of polyethylene oxide using diffusing wave spectroscopy and single scattering, Phys. Rev. E 65 (2002) 051505/1–051505/10.
[11] C.D. Chapman, K. Lee, D. Henze, D.E. Smith, R.M. Robertson-Anderson, Onset of non-continuum effects in microrheology of entangled polymer solutions, Macromolecules 47 (2014) 1181–1186.
[12] S. Köster, Y.C. Lin, H. Herrmann, D.A. Weitz, Nanomechanics of vimentin intermediate filament networks, Soft Matter 6 (2010) 1910–1914.
[13] M.A. Kotlarchyk, E.L. Botvinick, A.J. Putnam, Characterization of hydrogel microstructure using laser tweezers particle tracking and confocal reflection imaging, J. Phys.: Condens. Matter 22 (2010).
[14] A. Aufderhorst-Roberts, W.J. Frith, A.M. Donald, Micro-scale kinetics and heterogeneity of a pH triggered hydrogel, Soft Matter 8 (2012) 5940–5946.
[15] A. Aufderhorst-Roberts, W.J. Frith, A.M. Donald, A microrheological study of hydrogel kinetics and micro-heterogeneity, Eur. Phys. J. E 37 (2014) 1–11.
[16] A. Aufderhorst-Roberts, W.J. Frith, M. Kirkland, A.M. Donald, Microrheology and microstructure of Fmoc-derivative hydrogels, Langmuir 30 (2014) 4483–4492.
[17] D.J. Adams, M.F. Butler, W.J. Frith, M. Kirkland, L. Mullen, P. Sanderson, A new method for maintaining homogeneity during liquid-hydrogel transitions using low molecular weight hydrogelators, Soft Matter 5 (2009) 1856–1862.
[18] K. Schätzel, Accuracy of photon correlation measurements on nonergodic samples, Appl. Opt. 32 (1993) 3880–3885.
[19] F.K. Oppong, L. Rubatat, B.J. Frisken, A.E. Bailey, J.R. De Bruyn, Microrheology and structure of a yield-stress polymer gel, Phys. Rev. E 73 (2006).
[20] A.Z. Cardoso, A.E. varez Alvarez, B.N. Cattoz, P.C. Griffiths, S.M. King, W.J. Frith, D.J. Adams, The influence of the kinetics of self-assembly on the properties of dipeptide hydrogels, Faraday Discuss. 166 (2013) 101–116.
[21] A.M. Corrigan, A.M. Donald, Particle tracking microrheology of gel-forming amyloid fibril networks, Eur. Phys. J. E 28 (2009) 457–462.
[22] T.H. Larsen, E.M. Furst, Microrheology of the liquid–solid transition during gelation, Phys. Rev. Lett. 100 (2008).
[23] T.M. Squires, T.G. Mason, Fluid mechanics of microrheology, Ann. Rev. Fluid Mech. 42 (2010) 413–438.
[24] M.T. Valentine, P.D. Kaplan, D. Thota, J.C. Crocker, T. Gisler, R.K. Prud'Homme, M. Beck, D.A. Weitz, Investigating the microenvironments of inhomogeneous soft materials with multiple particle tracking, Phys. Rev. E 64 (2001) 061506/1–061506/9.
[25] B.R. Dasgupta, D.A. Weitz, Microrheology of cross-linked polyacrylamide networks, Phys. Rev. E 71 (2005).
[26] M. Doi, S.F. Edwards, The Theory of Polymer Dynamics, Oxford University Press, New York, 1986.
[27] R.G. Larson, The Structure and Rheology of Complex Fluids, Oxford University Press, New York, 2014.
[28] F. Gittes, F.C. MacKintosh, Dynamic shear modulus of a semiflexible polymer network, Phys. Rev. E 58 (1998) R1241–R1244.
[29] T.G. Mason, Estimating the viscoelastic moduli of complex fluids using the generalized Stokes–Einstein equation, Rheol. Acta 39 (2000) 371–378.
[30] J. Xu, A. Palmer, D. Wirtz, Rheology and microrheology of semiflexible polymer solutions: actin filament networks, Macromolecules 31 (1998) 6486–6492.
[31] M.A.K. Williams, R.R. Vincent, D.N. Pinder, Y. Hemar, Microrheological studies offer insights into polysaccharide gels, J. Non-Newton. Fluid Mech. 149 (2008) 63–70.
[32] J. Apgar, Y. Tseng, E. Fedorov, M.B. Herwig, S.C. Almo, D. Wirtz, Multiple-particle tracking measurements of heterogeneities in solutions of actin filaments and actin bundles, Biophys. J. 79 (2000) 1095–1106.
[33] I.Y. Wong, M.L. Gardel, D.R. Reichman, E.R. Weeks, M.T. Valentine, A.R. Bausch, D.A. Weitz, Anomalous diffusion probes microstructure dynamics of entangled F-actin networks, Phys. Rev. Lett. 92 (2004) 178101.